

ORIGINAL ARTICLE

Estimating contemporary effective population size in non-model species using linkage disequilibrium across thousands of loci

RK Waples^{1,3}, WA Larson^{1,4} and RS Waples²

Contemporary effective population size (N_e) can be estimated using linkage disequilibrium (LD) observed across pairs of loci presumed to be selectively neutral and unlinked. This method has been commonly applied to data sets containing 10–100 loci to inform conservation and study population demography. Performance of these N_e estimates could be improved by incorporating data from thousands of loci. However, these thousands of loci exist on a limited number of chromosomes, ensuring that some fraction will be physically linked. Linked loci have elevated LD due to limited recombination, which if not accounted for can cause N_e estimates to be downwardly biased. Here, we present results from coalescent and forward simulations designed to evaluate the bias of LD-based N_e estimates (\hat{N}_e). Contrary to common perceptions, increasing the number of loci does not increase the magnitude of linkage. Although we show it is possible to identify some pairs of loci that produce unusually large r^2 values, simply removing large r^2 values is not a reliable way to eliminate bias. Fortunately, the magnitude of bias in \hat{N}_e is strongly and negatively correlated with the process of recombination, including the number of chromosomes and their length, and this relationship provides a general way to adjust for bias. Additionally, we show that with thousands of loci, precision of \hat{N}_e is much lower than expected based on the assumption that each pair of loci provides completely independent information. *Heredity* (2016) **117**, 233–240; doi:10.1038/hdy.2016.60; published online 24 August 2016

INTRODUCTION

Effective population size (N_e) is a fundamental population genetics concept (Wright, 1931), which determines the rate of evolutionary change due to genetic drift and informs the equilibrium level of genetic variation and the effectiveness of selection. N_e is often much lower than census size (Frankham, 1995), demonstrating that simply counting individuals is insufficient to predict rates of evolutionary change. In addition to the number of mating individuals, N_e is affected by sex ratio, variation in reproductive success, age structure, migration and other demographic factors. It is an extremely relevant metric in conservation biology, with low N_e leading to inbreeding and reduced genetic diversity (Ellstrand and Elam, 1993). See Charlesworth (2009) for a primer on N_e , and Wang (2005) for a review of estimation methods.

Populations with smaller N_e undergo more genetic drift than larger populations. This genetic drift randomly generates associations between alleles at different loci, known as linkage (or gametic) disequilibrium (LD) at a rate inversely proportional to N_e . As a result, measures of LD between independently-segregating loci can be used to provide an estimate of N_e (Sved, 1971; Hill, 1981; Waples, 1991). Over the past decades, many studies have leveraged data sets consisting of a few dozen loci for genetic estimates of N_e (Luikart *et al.*, 2010). While these studies continue to be useful, especially for long-running

projects, biologists now have access to genomic methods that generate orders of magnitude more data. These technologies are growing quickly and have made it feasible to genotype many thousands of loci and improve inference of demographic parameters, provided that the scale and particularities of these new data sets are managed well. Here, we examine the benefits of applying the LD method to estimate contemporary N_e with high-throughput genomic data, and address implications for both bias and precision.

To estimate contemporary N_e with the LD method, it is necessary to measure LD between loci that are inherited independently (that is, recombination fraction (c) equal to 0.5). Estimates of past N_e are available by measuring LD between physically-linked loci with recombination fraction less than 0.5 (Hill, 1981); however, recombination fractions must be known with high precision to look more than a few generations in the past. Recombination fractions are rarely known for non-model species, so this effectively limits their application to model species (for example, Tenesa *et al.*, 2007; Hollenbeck *et al.*, 2016). For non-model species, a blanket assumption of no linkage among loci is often made. This assumption can be reasonable, as the chance that any two loci are physically linked is small, and many analyses are robust to a minor degree of ‘background’ LD (for example, Falush *et al.*, 2003). However, with data sets spanning thousands of loci, assuming a complete absence of physical linkage is

¹School of Aquatic and Fishery Sciences, University of Washington, Seattle, WA, USA and ²Northwest Fisheries Science Center, National Marine Fisheries Service, National Oceanic and Atmospheric Administration, Seattle, WA, USA

³Current address: Department of Biology, The Bioinformatics Centre, University of Copenhagen, 2200 Copenhagen, Denmark.

⁴Current address: College of Natural Resources, University of Wisconsin-Stevens Point, Stevens Point, WI, USA.

Correspondence: RK Waples, Department of Biology, The Bioinformatics Centre, University of Copenhagen, 2200 Copenhagen, Denmark.

E-mail: ryan.waples@gmail.com

Received 30 September 2015; revised 19 June 2016; accepted 24 June 2016; published online 24 August 2016

no longer tenable for methods that are sensitive to linkage, such as estimating relatedness (Thompson, 2013) and N_e .

Here, we empirically examine the bias of N_e estimation due to physical linkage in a simulation study designed to evaluate the common situation where a researcher has genomics-scale data sets (for example, 1000s of loci) but limited other genomic resources. We explore factors underlying bias in terms of genetic architecture and relate this bias to the number and length of chromosomes. We focus on the simple case of a single sample taken from a single population. Simulated data are generated using a 'sideways' approach that combines both coalescent and forward simulations. Coalescent simulations ensure equilibrium and allow simple modeling of ascertainment, while forward simulations provide precise control over important parameters such as mating structure. This hybrid simulation procedure allows us to explore and quantify the effect of these aspects on bias in N_e estimates.

We show that the presence of physically-linked loci downwardly biases estimates of contemporary N_e based on the LD method, and that basic aspects of genomic architecture, such as the number of chromosomes and genome size, influence the amount of physical linkage. For example, bias created by physical linkage decreases as the number of chromosomes increases, as larger genomes house more independently assorting loci. Using these gross measures of genome architecture and our simulated data, we develop approximate bias corrections to account for the effects of linkage. We illustrate our results by calculating biased and putatively unbiased estimates of N_e from a published data set that includes 28 populations of Atlantic salmon (*Salmo Salar*) sampled across their range in Europe and North America (Bourret *et al.*, 2013) and an Atlantic salmon linkage map. We also show that, although high-throughput sequencing techniques will increase precision of N_e estimates, the lack of independence of the vast numbers of pairwise comparisons means that precision in \hat{N}_e does not increase nearly as fast as naive expectation.

MATERIALS AND METHODS

Simulation procedure

Genetic data were generated in a two-step backward/forward procedure. First, a coalescent simulation program, SIMCOAL2 (Laval and Excoffier, 2004) was used to produce populations in approximate mutation-drift equilibrium. These populations were then used to initialize the forward-time simulation program SimuPop (Peng and Kimmel, 2005). In the forward simulation, populations were held to a 1:1 sex ratio with random mating. In this scenario, the expected N_e is equal to the census size (N), although the realized N_e varies each generation due to random fluctuation in family sizes (Waples and Faulkner, 2009).

The simulation procedure involved four nested steps, each replicated independently. (1) We created a genomic architecture, by randomly placing loci on chromosomes. (2) Informed by the genomic architecture, we used coalescent simulations to produce populations of constant size in mutation-drift-recombination equilibrium. (3) We initialized forward-time simulations with the coalescent results and progressed 10 generations forward in time,

without mutation. (4) In the final generation, we selected a subsample of individuals for analysis. See Supplementary materials for detailed information on the simulation procedure.

We were interested in evaluating bias and precision of estimates of N_e . To investigate bias due to physical linkage, we created simulation scenarios that varied the population size (50, 200, 800), number of loci (1024, 4096), number of chromosomes (2–64) and sample sizes of individuals (50, 100), in a fully factorial design (Table 1); see Supplementary materials for results for smaller numbers of loci. Generally, two parents were randomly selected to produce each offspring and simulated chromosomes were 100 centimorgans (cM) long, except where noted below. To examine the effect of chromosomes length and recombination rate on the bias, we re-ran a subset of scenarios (number of chromosomes = 4, 8) with both shortened (50 cM) and lengthened (200 cM) chromosomes. To examine precision of N_e estimates, we used a single parameter set with population size = 200, 8 chromosomes, 4096 loci, sample size = 100, and conducted 1000 forward simulations based on a single genomic architecture started from the same coalescent initialization and held the realized N_e constant each generation.

Notice that for a simulated population size of 50, no sample size of 100 is possible and that all samples of 50 individuals will be identical. For each genome created in step 1, steps 2, 3, and 4 were replicated 2, 10, and 4 times, respectively. This generally produced 80 replicates for each combination of parameters.

Estimation of N_e

N_e was estimated from the mean amount of LD present in the genome remaining after accounting for sampling-induced LD. We used PLINK ver. 1.07 (Purcell *et al.*, 2007) to calculate Pearson's squared correlation coefficient (r^2) of the genotype vectors for each pair of loci as a measure of LD. Genotypes were coded as the number of non-reference alleles, with possible values in [0, 1, 2]. With genotypes coded in this way, r^2 is identical to Burrows' composite measure of linkage disequilibrium (r_D) (Weir, 1996; Zaykin, 2004). To mirror the approach implemented in the software LDNe (Waples and Do, 2008), where a sample-size adjustment factor of $[S/(S-1)]^2$ was used (Weir, 1979), we multiplied each r^2 value by this term, subtracted the expected contribution from sampling error to obtain the adjusted r^2 , and then calculated \hat{N}_e as in Waples (2006).

For each simulation, mean r^2 was calculated as the mean across all pairs of loci. Other methods have computed a weighted mean based on allele frequencies, number of alleles and/or missing data (for example, Peel *et al.*, 2013; Sved *et al.*, 2013), but here we simulate only bi-allelic loci without missing data and did not compute a weighted mean. Alleles observed in low numbers (≤ 2) provide little information on LD and can upwardly bias estimates of r^2 (Waples and Do, 2010), so we excluded loci with an observed minor allele frequency of < 0.05 in each replicate. Using the LD method, after correcting for sampling-induced LD, it is possible to produce estimates of infinite N_e ; to incorporate these values into summary statistics we replaced infinite estimates with 10 000.

For each pair of loci, an expected value for r^2 ($E(r^2)$) was calculated as a function of N_e and c , the recombination fraction of the two loci. We used a hybrid of two different formulas for $E(r^2)$: equation 2 in Weir and Hill (1980) and equation 3 in Sved and Feldman (1973). The Sved and Feldman formula is incorrect for unlinked loci ($c = 0.5$) (Sved *et al.*, 2013), while the Weir and Hill (1980) formula produces non-sensical values ($E(r^2) > 1$) for closely linked loci.

Table 1 Simulation parameters and replication, full factorial design, all possible combinations of parameters were simulated

Simulation type	Simulation parameters				Replication			
	# Loci	# Chrs	N	Sample size	Coalescent	Forward	Sampling	Total replicates
Bias	1024, 4096	2, 4, 8, 16, 32, 64	50, 200, 800	50, 100 ^a	2	10	4	80
Precision	16, 32, 64, 128, 256, 512, 1024, 2048, 4096	8	200	100	1	1000	1	1000

^aFor a simulated population size of 50, no sample size of 100 is possible, and replication across sample sizes of 50 is not meaningful. N is the number of simulated individuals.

Accordingly, we used the minimum $E(r^2)$ across the two equations. See supplementary Figure S1 for an illustration of the relationship between $E(r^2)$ and c for each equation.

For pairs of bi-allelic loci observed within a population, the statistic (r^2 /mean (r^2)) follows a chi-squared distribution with one degree of freedom (Hill, 1981). To form the $E(r^2)$ distribution for pairs of loci with a known recombination fraction, we re-scaled the chi-squared distribution to have a mean equal to $E(r^2)$ and bounded it at 1.0. This allowed us to evaluate the extent to which the empirical distribution of r^2 within our simulations departed from the expected values. To form a distribution of $E(r^2)$ for many pairs of loci with different values for c , we computed a weighted sum of their expected distributions. Using this approach, we were able to closely approximate the empirical distribution of pairwise r^2 values, matching the $E(r^2)$ distribution for both unlinked loci and across the full range of simulated recombination fractions (Supplementary Figure S2).

Bias

LD between neutral and independently-segregating loci should provide a nearly unbiased estimate of N_e (Hill, 1981; Waples and Do, 2010). Bias in N_e estimates was assessed by comparing estimates with census sizes (N) of Wright–Fisher ideal populations. We evaluated this bias before and after excluding within-chromosome comparisons from LD measurements. This method leverages our complete knowledge of the genomic architecture in the simulated data, and allows an assessment of estimates of N_e based on r^2 for all pairs of loci (biased by physical linkage) to estimates derived from the mean r^2 for pairs of loci on different chromosomes (unbiased by physical linkage). Any increase in bias based on the within-chromosome LD measures can be attributed to physical linkage between loci.

In addition to characterizing the degree of bias, we evaluated two types of bias correction methods: (1) set a cutoff r^2 value and exclude all pairwise r^2 values above it from the calculation of mean r^2 and (2) adjust estimates of N_e directly based on the number of chromosomes or their total genetic length in cM.

Empirical example

While simulations are ideal at replicating simple scenarios, real populations have many complexities not matched in simulated data. To investigate how the above methods can be applied to real populations, genetic data from 28 populations of Atlantic salmon (Bourret *et al.*, 2013) were used to estimate N_e . From the published data set, we excluded populations with mean sample sizes <30 and samples that combined individuals from multiple years, as these issues can also bias estimates of N_e (Waples *et al.*, 2014). We restricted our analysis to loci present on the linkage map of Lien *et al.* (2011) and the linkage groups of this map were treated as chromosomes. Any loci identified by Bourret *et al.* (2013) as putatively under selection, or with minor allele frequency <0.05 , were excluded. We placed the r^2 values for each pair of loci into sets of ‘unlinked’ (loci on different chromosomes), and ‘linked’ (loci co-located on a chromosome) following Larson *et al.* (2014). Mean r^2 within the ‘unlinked’ set provides an unbiased estimate of contemporary N_e , while the mean r^2 across both sets represents a naive approach blind to the effects of the physical linkage. This naive approach mirrors the lack of genomic resources, such as a reference genome or linkage map, that is present in most non-model species and in nearly all species of conservation concern. N_e estimates were generated with a custom version of the LDNe program (Waples and Do, 2008) available from the authors upon request. This estimation procedure closely matches the calculations made in the analysis of the simulated data, except a weighted mean r^2 was calculated based on the sample size of each locus due to some missing data.

Our simulations model simplified scenarios in which all chromosomes are the same length in cM and have the same number of ascertained loci. In real species, recombination (and thus chromosome length in cM) varies, thus we applied bias corrections for the Atlantic salmon data that incorporate both the size and number of linkage groups. These two bias corrections require different degrees of knowledge about genome structure and reflect the range of commonly-available information for non-model species.

Precision

Due to a limited number of recombination events each generation, loci do not segregate independently. This lack of independence between loci, coupled with the fact that each locus contributes to many pairwise r^2 measurements, is not accounted for when generating standard confidence intervals (CIs) around the mean r^2 or \hat{N}_e . To evaluate how much these effects reduce precision, we conducted a separate round of simulations and compared two measures of confidence: (1) nominal CIs around \hat{N}_e that assume all pairwise comparisons of loci are independent (Waples, 2006) and (2) empirical 95% intervals observed in the simulated data. Forward simulations of populations following a random Wright–Fisher mating model produce random variation in realized N_e as the variance in reproductive success varies each generation, even if census size stays constant. This inflates the variance of \hat{N}_e among replicate forward simulations (Waples and Faulkner, 2009). In most cases, this variation is confounded with other sampling processes, making it difficult to independently quantify them all. Therefore, for the simulations evaluating precision, we departed from a fully-random Wright–Fisher mating model and instead manually controlled mating to ensure that the realized variance in reproductive success was equal to the binomial variance, so that realized effective size was equal to the census size each generation. This excluded demographic fluctuations in realized N_e and allowed us to attribute all the variance of mean r^2 values among replicates to the processes of sampling individuals and loci. These manually-controlled matings were specified by randomly permuting individuals across a pedigree known to produce the desired N_e .

RESULTS

Bias

Within a chromosome, the distribution of locus pairs with a given recombination fraction is independent of the number of loci (Figure 1). Expected LD is a function of recombination fraction, so increasing the number of loci does not change the expected pattern or magnitude of LD. Because separate chromosomes segregate independently, increasing the number of loci does not increase the expected fraction of locus pairs that are physically linked. Although this result is not necessarily intuitive, it follows directly from the fact that the probability that any randomly-chosen pair of loci is linked is the same regardless how many other loci exist. Consistent with this expectation, the absolute number of loci measured was not found to have any systematic effect on estimates of mean r^2 or on estimates of N_e (Supplementary Figure S3). See Supplementary Table S1 for a summary of each simulation.

Although bias in \hat{N}_e depends to a limited extent on population size and sample size (see Supplementary Figure S4), by far the

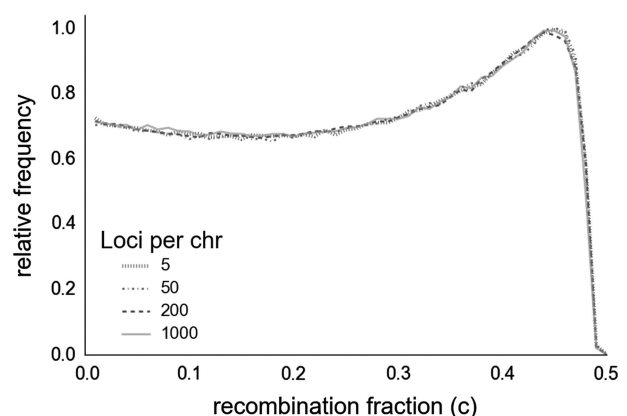


Figure 1 The distribution of recombination fractions among pairs of loci on a simulated chromosome. Simulated chromosomes are 100 cM in length; loci at opposite ends have c values near 0.5.

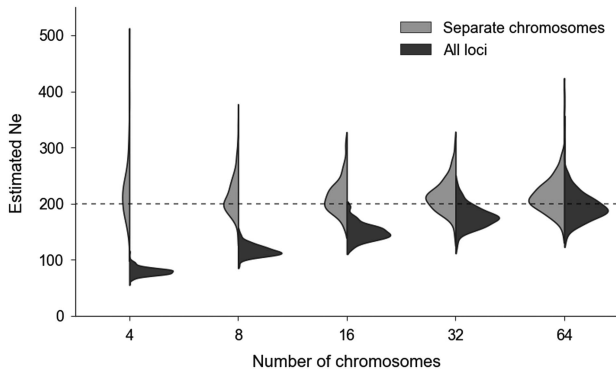


Figure 2 Relationship between bias in \hat{N}_e and the number of haploid chromosomes. The distribution of \hat{N}_e from all loci is shown in dark shading; estimates using only unlinked loci are shown in light shading. The horizontal dashed line shows the simulated population size.

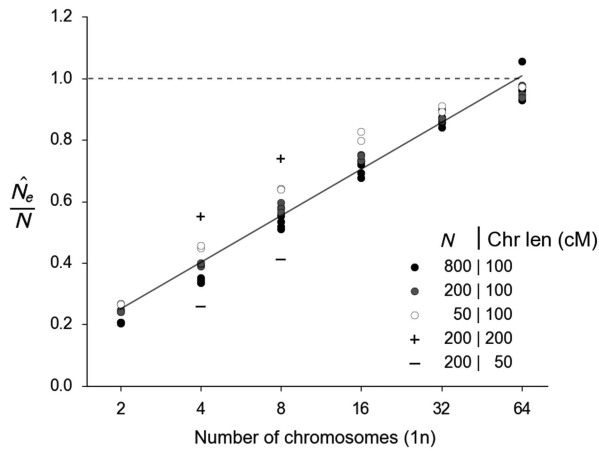


Figure 3 Pattern of bias in \hat{N}_e for simulated data as a function of the number haploid chromosomes. Results are based on mean r^2 values computed across all pairs of loci. Symbols are harmonic means of \hat{N}_e/N_e across all replicates for each parameter set. The solid line is a linear regression of \hat{N}_e/N_e on the natural log of the number of chromosomes (Chr): $y = 0.098 + 0.219 \times \ln(Chr)$. Plus symbols show results from simulations with $N = 200$ with longer chromosomes (200 cM) for the 4 and 8 chromosome scenarios; minus symbols show the effects of shorter chromosomes (50 cM). Dashed line is the relationship between the harmonic mean of \hat{N}_e and N for an unbiased estimate.

strongest indicator of the \hat{N}_e/N_e ratio is the number of chromosomes and their length in cM (Figures 2 and 3, Supplementary Table S2). This bias is caused by physically-linked loci and can be substantial. For example, with four chromosomes of 100 cM, the bias in \hat{N}_e is about -60% of true N_e , with slightly less bias associated with small populations. With 32 chromosomes, however, the bias in \hat{N}_e is reduced to about $-10\text{--}20\%$. We also see that the chromosome length in cM (proportional to the expected number of recombination events per generation) also has an effect, with eight 50 cM chromosomes generating a similar degree of bias to four 100 cM chromosomes (Figure 3). This suggests that the bias is a function of the total length of the genome in cM.

We considered an initial approach to bias adjustment that is analogous to the identification of 'outlier' loci that show levels of genetic differentiation among populations that are not consistent with

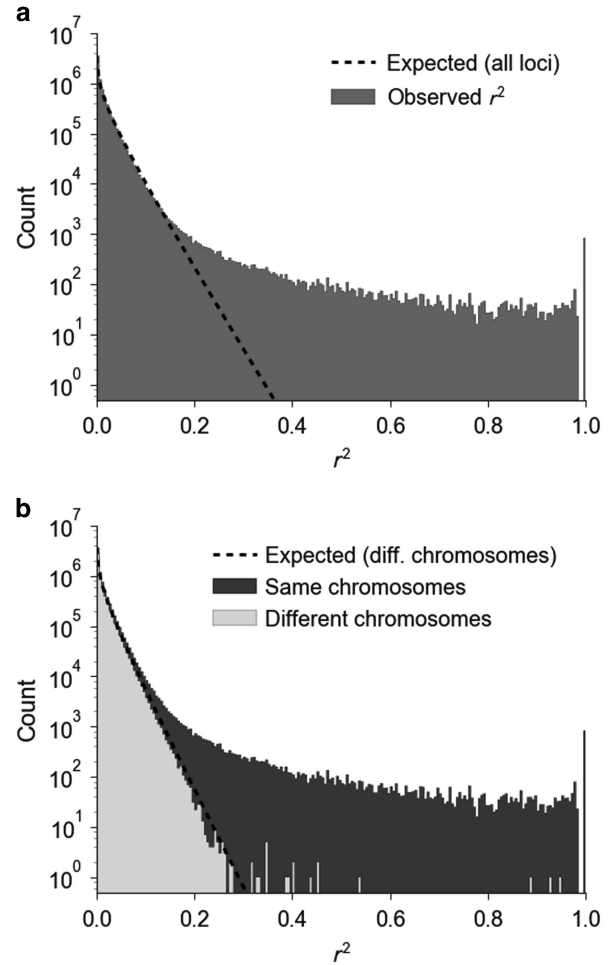


Figure 4 (a) is a histogram of r^2 values across all loci. The 'expected' line is calculated from the overall mean r^2 . (b) is a stacked histogram and separates the same data into within-chromosome (dark) and between-chromosome (light) r^2 measurements. The 'expected' line is calculated from the mean r^2 of all between-chromosome values. Data presented are from a simulation with population size = 200, with 4096 loci on 8 chromosomes, and a sample size of 100. Note the log-scaled y-axis.

neutral genetic drift (Beaumont and Nichols, 1996). With limited information about genomic architecture, from the mean r^2 across all pairs of loci one can compute the expected distribution of r^2 values for individual pairs of loci, under the assumption that they all are unlinked (see Materials and methods). This expected distribution can be compared with the observed r^2 values to identify r^2 values unlikely to occur for unlinked loci. Figure 4 shows the distribution of r^2 values for comparisons of 4096 loci on 4 chromosomes in a population of size $N = 200$ and a sample size of 100 individuals. Figure 4a shows the raw data with the r^2 measurements from linked and unlinked loci confounded, and the black dashed line shows the expected distribution of r^2 values under the assumption that all locus pairs are unlinked and therefore come from a single distribution. Figure 4b breaks down the data from (Figure 4a) into within- and between-chromosome measurements. The distribution of r^2 values for co-located loci is right-shifted compared with unlinked loci, but there is still significant overlap. The fit of the expected distribution to the unlinked loci (Figure 4b) is very good. In contrast, when all locus pairs

are used (Figure 4a), there is an excess of large r^2 values compared with the expectation.

We explored various criteria for defining a threshold for truncating unusually large r^2 values that presumably reflect linkage and hence will downwardly bias estimates of N_e . Figure 5 shows results of applying a threshold X to small bins of r^2 values such that bins for which the ratio of the number of observed to expected r^2 values was larger than X were removed. Using a more stringent threshold (X closer to 1) was more effective in reducing bias, but we found a strong asymptotic effect that limits effectiveness of the bias adjustment. Even using a stringent $X = 1.1$ criterion, downward bias in \hat{N}_e/N_e was only reduced from -67% for no adjustment to -40% for simulations with 4 chromosomes, and from -25 to -11% for simulations with 16 chromosomes. This one-pass truncation method is safe, in the sense that it does not have an appreciable effect on data that have no linked loci, but it is also conservative in that it only removes part of the bias (Gruenthal *et al.*, 2014; Candy *et al.*, 2015; Stockwell *et al.*, 2016). We also evaluated iterative truncation methods, whereby mean r^2 is recalculated after removing the outlier pairs of loci and the new expected distribution is used to identify more outliers. However, this iterative approach is not conservative and is prone to overshooting the bias reduction and excluding many r^2 values that legitimately arise from unlinked loci (data not shown).

Without information on the chromosome placement of loci, it is not possible to fully determine whether two loci are co-located based on LD. Figure 4 illustrates the impossibility of fully removing the bias in \hat{N}_e from any truncation method based on the overall mean r^2 . Ideally, we want to identify and exclude r^2 values generated by linked loci. However, because of the large overlap in the distribution of r^2 values for linked and unlinked comparisons, any fixed truncation threshold will either fail to remove many linked comparisons (many false negatives) or will remove many valid comparisons of loci on different chromosomes (many false positives).

A second, and more promising, approach is to take advantage of the strong correlation between the magnitude of bias in \hat{N}_e/N_e and the number of chromosomes and genome length in cM (Figures 2 and 3).

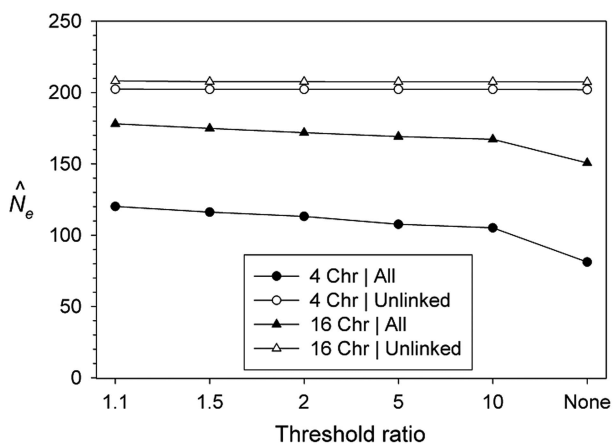


Figure 5 Effectiveness of removing outlier r^2 values to reduce bias. Results are shown for simulations with 4 and 16 chromosomes and estimates based on all loci (biased downwards) or only pairs of loci on different chromosomes ('unlinked'; little or no bias with respect to true $N_e = 200$). For each scenario, the expected distribution of pairwise r^2 values was generated based on the overall mean r^2 . Values on the x axis are different ratios of observed/expected r^2 values that were used to truncate the distribution, after which mean r^2 and \hat{N}_e were recalculated.

The relationship shown in Figure 3 can be used to generate a rough estimate of the magnitude of downward bias in \hat{N}_e due to physical linkage. In this figure, the symbols represent harmonic means of \hat{N}_e/N_e across 80 replicate simulations for each parameter set, with \hat{N}_e calculated from mean r^2 across all pairs of loci. The solid line is the least-squares regression of \hat{N}_e/N_e on the natural log of the number of chromosomes (Chr):

$$\frac{\hat{N}_e}{N_e} = 0.098 + 0.219 \times \ln(Chr) \quad (1a)$$

which explains 97% of the variance in these harmonic mean estimates. Accounting for sample size ($S = 50$ or 100) did not significantly improve the fit. Adding a term for $\ln(N_e)$ led to a statistically significant improvement ($P < 0.01$) that, however, led to only a negligible ($< 1\%$) increase in adjusted R^2 . This weak dependence of the bias on true N_e is convenient because N_e is the quantity we are trying to estimate. Thus, a simple, quantitative adjustment for bias in an estimate of N_e can be achieved by inserting the haploid chromosome number into Equations (1a) and (1b) and dividing the naive \hat{N}_e estimate by the regression result.

Alternatively, we can specify the total length of the genome in cM to predict the bias.

$$\frac{\hat{N}_e}{N_e} = -0.910 + 0.219 \times \ln(\text{cM}) \quad (1b)$$

Equation (1b) differs from Equation (1a) only in the constant term. In our simulations, each chromosome was 100 cM in length, but real species will have chromosomes of variable length.

Empirical example

We examine how the bias correction procedure developed above can be applied to data from natural populations: 28 populations of Atlantic salmon from across their range. Importantly, a linkage map in Atlantic salmon (Lien *et al.*, 2011) supplies chromosomal information for each locus. Across the populations investigated, mean naive \hat{N}_e was 255, range = 15–1801, s.d. = 406. Mean bias-corrected \hat{N}_e based on loci not co-located on chromosomes was 834, range = 18–10 000, s.d. = 2016. Figure 6 shows the effect of removing within-chromosome LD from N_e estimates. For all populations, mean r^2 was lower and \hat{N}_e was larger after excluding co-located loci. The female linkage map has 29

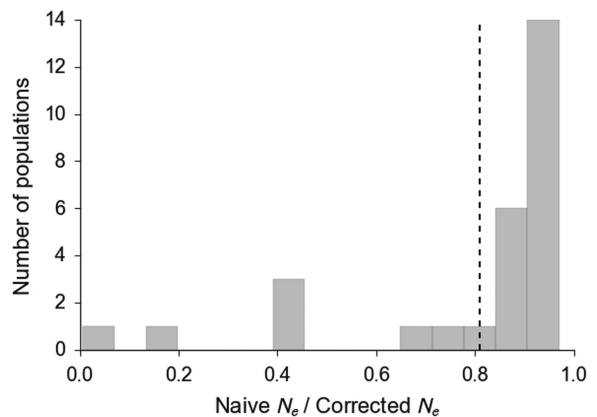


Figure 6 Effect of removing within-chromosome LD from N_e estimates in 28 Atlantic salmon populations. Values on x axis are the ratio of \hat{N}_e for naive (all locus comparisons) and corrected comparisons (only among loci on different chromosomes). Dashed line shows the predicted correction level based on 29 chromosomes.

(haploid) chromosomes and a total length of 2402 cM. Based on Equation (1a), we expect that N_e estimates for a species with 29 haploid chromosomes should be approximately the fraction $-0.910 + 0.219 \times \ln(29) = 0.83$ of true N_e , indicating an expected downward bias of 17%. Alternatively, using the genome length in cM 2402, Equation (1b) predicts a bias of $-0.910 + 0.219 \times \ln(2402) = 0.79$ of true N_e , indicating an expected downward bias of 21%. Using the correction based on knowledge of genomic location of each locus, the geometric mean of the downward bias in the Atlantic salmon data is 34.5% and the median is 9.8%. Our estimates are between these two measures of the central tendency of the bias. Most of the populations fell in the range of 0–20% downward bias (0.8–1.0, Figure 6, Supplementary Table S3), consistent with a moderate amount of downward bias. The populations with larger naive estimates of N_e in general had larger corrections (Supplementary Figure S5), consistent with Figure 3.

Precision

The precision of estimates of N_e is grossly overestimated when large numbers of loci are observed (Figure 7). For example, with 4096 loci and true $N_e = 200$, under the assumption that all comparisons are independent (that is, mean r^2 is the result of $\binom{4096}{2} = 8\,386\,560$ independent measures), the parametric 95% CI on the point estimate of \hat{N}_e (202) is extremely small: (201–203, Supplementary Table S4). In contrast, we show that in simulations of 4096 loci on 8 chromosomes we achieve empirical 95% intervals for \hat{N}_e that are equivalent to those produced by only 160 fully independent loci (that is, $\binom{160}{2} = 12\,720$ independent measures). The empirical 95% interval is 20 times wider (168–242) than this naive assumption, indicating that the effective degrees of freedom associated with the point estimate are only a fraction of the nominal degrees of freedom. This overly optimistic precision implied by the naive CI is especially egregious as the parametric CI is so narrow that it does not even include the true population size of 200, even though the point estimate is off by only 1%.

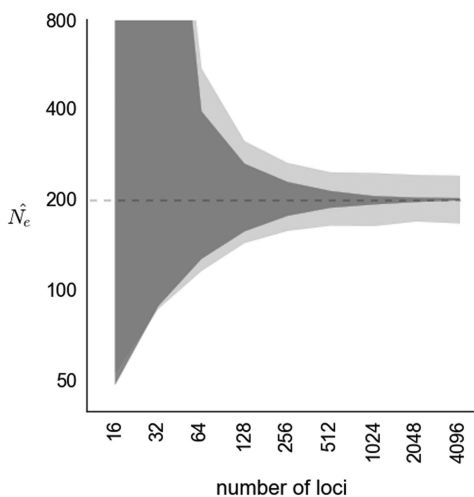


Figure 7 Relationship between theoretical and empirical (light) precision for estimates of N_e . Dark shaded area shows naive 95% CIs (which assume that all pairwise comparisons are independent), light shaded area shows empirical CIs from simulated data. True N_e was 200, sample size was 100 and number of chromosomes was 8. Notice both the x and y axes are log-scaled.

DISCUSSION

Implications for genomic data sets

Observing more loci does not increase the probability that any randomly-chosen pair of loci will be linked, nor increase the fraction of loci that are physically linked. However, as the number of loci increases, the fraction of pairs that are linked will converge on the expected fraction, which means that results are easier to predict in a statistical sense.

We showed how to compare the observed distribution of r^2 estimates for pairs of loci with the expected distribution under the assumption that all are neutral and unlinked. With this approach, it is easy to identify outlier pairs of loci with r^2 values that are unlikely to be generated under the assumed model. We explored various criteria for one-pass truncation of the r^2 values and showed that this approach can only be partially effective at reducing the downward bias in \hat{N}_e . The problem with this approach is that physical linkage encompasses the full range of recombination fractions from 0.5 to near zero. Only a relatively small number of strongly-linked loci produce outlier r^2 values above any given threshold, while vastly more pairs of loosely linked loci create slightly elevated r^2 values that cumulatively contribute to bias but cannot be easily distinguished from unlinked pairs that produce similar r^2 values.

Here, we are cognizant of the benefits of simplicity and recognize the lack of genomic resources for many species. In the simulated data, the relationship between downward bias in \hat{N}_e and chromosome length/number is nearly log-linear (Figure 3). For example, eight 200 cM chromosomes results in less bias than eight 50 cM chromosomes, but a similar amount of bias to 16 100 cM chromosomes. The simplest adjustment based on the number of chromosomes (Equation 1a) assumes an average of 100 cM per chromosome. With more detailed information on recombination rates, it is possible to incorporate relative lengths of chromosomes into the bias correction as well (Equation 1b).

This method should improve estimates of downward bias in \hat{N}_e for species with limited genomic resources. Realistically, the pattern of bias in \hat{N}_e due to physical linkage is constrained to the range 0–1, so the relationship depicted in Figure 3 must be sigmoidal as the bias asymptotes near these boundaries. Therefore, we do not suggest using Equations (1a) and (1b) to correct for bias outside the range of the simulated data here, that is, 2–64 chromosomes, 200–6400 cM. Within that range, however, the pattern of bias is nearly log-linear and hence amenable to correction using this simple adjustment.

We see a very slight upward bias in \hat{N}_e when applying the LDNe estimation method to sets of loci on different chromosomes. This effect is larger with smaller sample sizes (S). This has been noted previously (for example, Waples and Do, 2010) and is likely due to a slight bias overcorrection in LDNe method relative to the original Hill method. Our results thus allow the user to simultaneously correct for bias due to linkage and the slight upward bias that occurs in LDNe. Besides drift and physical linkage, other factors affecting LD include selection, migration and admixture (Slatkin, 2008). The LD generated by these other evolutionary forces also has the potential to bias estimates of N_e (Waples and England, 2011; Gilbert and Whitlock, 2015). The simulations conducted here, while extensive, were limited in many respects and did not attempt to address these forces. Specifically, we simulated isolated populations of constant size. The simulated genome architecture was also greatly simplified; all chromosomes were the same size, measured in recombination units and loci were distributed randomly with respect to local recombination rate and were strictly neutral.

In this study, we simulated loci that are randomly placed on chromosomes. However, both biological and methodological factors

may conspire to produce loci that are non-randomly distributed with respect to recombination. Many genotyping-by-sequencing methods, such as those based on restriction enzymes, are likely to produce loci that are closer together than random expectation. We note this may contribute to excess LD and further downward bias in N_e estimates, but we do not examine this further.

We evaluated our suggested approach with a published genetic data set of 28 populations of Atlantic salmon. Given 29 haploid chromosomes, our simulations predict there should be a downward bias in \hat{N}_e of about 17% (Figure 3). Alternatively, using the total length of the linkage map (2402 cM), our simulations predict a downward bias \hat{N}_e of about 21%. These corrections are conservative relative to the correction we observed by excluding loci co-located on chromosomes (geometric mean 34.5%). Although we do not know the true N_e of these populations and therefore cannot determine the true bias, we found that N_e always increased when comparisons of loci on the same chromosome were excluded, which clearly demonstrates the potential for bias. The populations with large corrections (>50%) were mostly for populations already estimated to be large, where precise estimation of N_e is known to be difficult; furthermore, some of the samples could be affected by admixture associated with artificial propagation or other anthropogenic factors not considered here.

The number of possible LD measurements increases with the square of the number of loci, so large genomics data sets vastly increase the number of pairwise r^2 values that are available to estimate N_e . However, because these comparisons are not all independent, precision is greatly reduced from the theoretical value. Previously, this problem of assessing precision for the LD method has been pointed out and illustrated with small numbers of loci (Waples, 2006; Waples and Do, 2010). We show that the magnitude of this problem increases dramatically for genomics-scale data sets, to the extent that realized precision will be much less than predicted from standard models that assume complete independence among loci. This is an important topic that merits a more detailed treatment than we can provide here. In the meantime, users should be aware that precision is greatly overestimated for large numbers of loci if CIs are generated under the assumption that all pairwise comparisons are independent.

Related approaches

We found a consistent increase in \hat{N}_e when loci known to be physically linked are excluded, in both simulated and wild populations. In contrast, in the Queensland fruit fly (*Bactrocera tryoni*), Sved *et al.* (2013) did not find a consistent change in \hat{N}_e across a set of ~30 microsatellite loci when co-located loci were excluded. This difference may be due to increased number of loci in this study, and/or the simplified nature of simulated data, both of which can tend to reduce noise in estimates. Our results are consistent with those of Larson *et al.* (2014), who showed a significant increase in \hat{N}_e in multiple populations of Chinook salmon (*Oncorhynchus tshawytscha*) when co-located single-nucleotide polymorphism loci were removed from analyses, the expected pattern if \hat{N}_e was downwardly biased by linkage. Notably, in all three studies of wild populations (*B. tryoni*, and two salmonids), the degree of difference in unlinked vs all estimates was not consistent across populations, suggesting population-specific factors that affect within-chromosome LD, such as historic bottlenecks and recent metapopulation dynamics (Slatkin, 2008), could have important implications for estimating contemporary N_e .

There are other methods available to estimate recent effective population size from genetic data. However, most of these methods require data types not available in many species. When available, genetic samples spaced in time can powerfully inform estimates of genetic drift

and thus N_e , for example, SPATPG (Gompert, 2016). With a detailed recombination map, equations relating the recombination fraction to expectations of LD can be used to estimate the recent history of N_e , for example, SNeP (Barbato *et al.*, 2015) and Hollenbeck *et al.* (2016). Finally, with dense, phased genotype data, powerful new methods allow inference of complex demographic histories, including N_e , for example, the multiple sequentially markovian coalescent (Schiffels and Durbin, 2014) and diCal (Sheehan *et al.*, 2013), but these data are not yet available for most species.

Practical applications

N_e estimates are useful in planning conservation actions and assessing genetic risk, and bias in N_e estimates can lead to inappropriate conservation decisions (Schwartz *et al.*, 2007). For conservation applications, not correcting for the bias demonstrated here can be seen as conservative, as it will result in the prediction of smaller N_e , but it could lead to false alarms that waste scarce resources on populations that are not actually at high genetic risk.

For species without many genomic resources, the most reliable means of adjusting bias in \hat{N}_e related to linkage is to use a correction factor based on the number of chromosomes or their total length in cM. With knowledge of the chromosome location of each locus, either from a linkage map or reference genome, it is possible to correct for the downward bias in N_e estimates. Although reference genomes are not available for most non-model species, a researcher will often know the number of chromosomes. In cases where this chromosomal information is lacking, the relationship given in Equations (1a) and (1b) and shown in Figure 3 can be used to partially correct for this bias. In both cases, we suggest practitioners exclude any loci expected to be under selection from use as estimators of N_e . The results and conclusions presented are relevant for studies that leverage LD to estimate contemporary N_e with any number of loci.

DATA ACCESSIBILITY

This study contains no new empirical data. The scripts used in the simulation analyses are available in Dryad (<http://dx.doi.org/10.5061/dryad.1ms70>). Atlantic salmon data were accessed from Dryad repository: doi:10.5061/dryad.gm367 (Bourret *et al.*, 2012).

CONFLICT OF INTEREST

The authors declare no conflict of interest.

ACKNOWLEDGEMENTS

We would like to thank Chi Do for making available a beta version of LDNE that facilitated computation of mean r^2 across loci on different chromosomes. RKW was supported by the Alaska Sustainable Salmon Fund under Projects 44714 and 44812 from the National Oceanic and Atmospheric Administration, US Department of Commerce, administered by the Alaska Department of Fish and Game. WAL was supported by the H Mason Keeler Endowment for Excellence and a US National Science Foundation Graduate Research Fellowship (grant # DGE-0718124).

AUTHOR CONTRIBUTIONS

RSW conceived the study, along with RKW and WAL. RKW conducted all simulations. RKW, WAL and RSW analyzed data; writing and editing the manuscript was conducted by RKW with help from WAL and RSW.

Barbato M, Orozco-terWengel PA, Tapio M, Bruford MW (2015). SNeP: a tool to estimate trends in recent effective population size trajectories using genome-wide SNP data. *Front Genet* 6: 109.

- Beaumont MA, Nichols RA (1996). Evaluating loci for use in the genetic analysis of population structure. *Proc R Soc B* **263**: 1619–1626.
- Bourret V, Kent MP, Primmer CR, Vasemägi A, Karlsson S, Hindar K *et al.* (2013). SNP-array reveals genome-wide patterns of geographical and potential adaptive divergence across the natural range of Atlantic salmon (*Salmo salar*). *Mol Ecol* **22**: 532–551.
- Bourret V, Kent MP, Primmer CR, Vasemägi A, Karlsson S, Hindar K *et al.* (2012). Data from: SNP-array reveals genome wide patterns of geographical and potential adaptive divergence across the natural range of Atlantic salmon (*Salmo salar*). *Mol Ecol* **22**: 532–551.
- Candy JR, Campbell NR, Grinnell MH, Beacham TD, Larson WA, Narum SR (2015). Population differentiation determined from putative neutral and divergent adaptive genetic markers in Eulachon (*Thaleichthys pacificus*, Osmeridae), an anadromous Pacific smelt. *Mol Ecol Resour* **15**: 1421–1434.
- Charlesworth B (2009). Fundamental concepts in genetics: effective population size and patterns of molecular evolution and variation. *Nat Rev Genet* **10**: 195–205.
- Ellstrand NC, Elam DR (1993). Population genetic consequences of small population-size – implications for plant conservation. *Annu Rev Ecol Syst* **24**: 217–242.
- Falush D, Stephens M, Pritchard JK (2003). Inference of population structure using multilocus genotype data: linked loci and correlated allele frequencies. *Genetics* **164**: 1567–1587.
- Frankham R (1995). Effective population-size adult-population size ratios in wildlife – a review. *Genet Res* **66**: 95–107.
- Gilbert KJ, Whitlock MC (2015). Evaluating methods for estimating local effective population size with and without migration. *Evolution* **69**: 2154–2166.
- Gompert Z (2016). Bayesian inference of selection in a heterogeneous environment from genetic time-series data. *Mol Ecol* **25**: 121–134.
- Gruenthal KM, Witting DA, Ford T, Neuman MJ, Williams JP, Pondella II DJ *et al.* (2014). Development and application of genomic tools to the restoration of green abalone in southern California. *Conserv Genet* **15**: 109–121.
- Hill WG (1981). Estimation of effective population-size from data on linkage disequilibrium. *Genet Res* **38**: 209–216.
- Hollenbeck CM, Portnoy DS, Gold JR (2016). A method for detecting recent changes in contemporary effective population size from linkage disequilibrium at linked and unlinked loci. *Heredity*, **117**: 207–216.
- Larson WA, Seeb LW, Everett MV, Waples RK, Templin WD, Seeb JE (2014). Genotyping by sequencing resolves shallow population structure to inform conservation of Chinook salmon (*Oncorhynchus tshawytscha*). *Evol Appl* **7**: 355–369.
- Laval G, Excoffier L (2004). SIMCOAL 2.0: a program to simulate genomic diversity over large recombining regions in a subdivided population with a complex history. *Bioinformatics* **20**: 2485–2487.
- Lien S, Gidskehaug L, Moen T, Hayes BJ, Berg PR, Davidson WS *et al.* (2011). A dense SNP-based linkage map for Atlantic salmon (*Salmo salar*) reveals extended chromosome homeologies and striking differences in sex-specific recombination patterns. *BMC Genomics* **12**: 615.
- Luikart G, Ryman N, Tallmon DA, Schwartz MK, Allendorf FW (2010). Estimation of census and effective population sizes: the increasing usefulness of DNA-based approaches. *Conserv Genet* **11**: 355–373.
- Peel D, Waples RS, Macbeth GM, Do C, Ovenden JR (2013). Accounting for missing data in the estimation of contemporary genetic effective population size (N_e). *Mol Ecol Resour* **13**: 243–253.
- Peng B, Kimmel M (2005). simuPOP: a forward-time population genetics simulation environment. *Bioinformatics* **21**: 3686–3687.
- Purcell S, Neale B, Todd-Brown K, Thomas L, Ferreira MA, Bender D *et al.* (2007). PLINK: a tool set for whole-genome association and population-based linkage analyses. *Am J Hum Genet* **81**: 559–575.
- Schiffels S, Durbin R (2014). Inferring human population size and separation history from multiple genome sequences. *Nat Genet* **46**: 919–925.
- Schwartz MK, Luikart G, Waples RS (2007). Genetic monitoring as a promising tool for conservation and management. *Trends Ecol Evol* **22**: 25–33.
- Sheehan S, Harris K, Song YS (2013). Estimating variable effective population sizes from multiple genomes: a sequentially Markov conditional sampling distribution approach. *Genetics* **194**: 647–662.
- Slatkin M (2008). Linkage disequilibrium – understanding the evolutionary past and mapping the medical future. *Nat Rev Genet* **9**: 477–485.
- Stockwell BL, Larson WA, Waples RK, Abesamis RA, Seeb LW, Carpenter KE (2016). The application of genomics to inform conservation of a functionally important reef fish (*Scarus niger*) in the Philippines. *Conserv Genet* 1–11.
- Sved JA (1971). Linkage disequilibrium and homozygosity of chromosome segments in finite populations. *Theor Popul Biol* **2**: 125–141.
- Sved JA, Cameron EC, Gilchrist AS (2013). Estimating effective population size from linkage disequilibrium between unlinked loci: theory and application to fruit fly outbreak populations. *PLoS One* **8**: e69078.
- Sved JA, Feldman MW (1973). Correlation and probability methods for one and two loci. *Theor Popul Biol* **4**: 129–132.
- Tenesa A, Navarro P, Hayes BJ, Duffy DL, Clarke GM, Goddard ME *et al.* (2007). Recent human effective population size estimated from linkage disequilibrium. *Genome Res* **17**: 520–526.
- Thompson EA (2013). Identity by descent: variation in meiosis, across genomes, and in populations. *Genetics* **194**: 301–326.
- Wang J (2005). Estimation of effective population sizes from data on genetic markers. *Philos Trans R Soc Lond B Biol Sci* **360**: 1395–1409.
- Waples RS (1991). Genetic methods for estimating the effective size of cetacean populations. *Report - International Whaling Commission, Special Issue* **13**: 279–300.
- Waples RS (2006). A bias correction for estimates of effective population size based on linkage disequilibrium at unlinked gene loci. *Conserv Genet* **7**: 167–184.
- Waples RS, Antao T, Luikart G (2014). Effects of overlapping generations on linkage disequilibrium estimates of effective population size. *Genetics* **197**: 769–780.
- Waples RS, Do C (2008). Idne: a program for estimating effective population size from data on linkage disequilibrium. *Mol Ecol Resour* **8**: 753–756.
- Waples RS, Do C (2010). Linkage disequilibrium estimates of contemporary N_e using highly variable genetic markers: a largely untapped resource for applied conservation and evolution. *Evol Appl* **3**: 244–262.
- Waples RS, England PR (2011). Estimating contemporary effective population size on the basis of linkage disequilibrium in the face of migration. *Genetics* **189**: 633–644.
- Waples RS, Faulkner JR (2009). Modelling evolutionary processes in small populations: not as ideal as you think. *Mol Ecol* **18**: 1834–1847.
- Weir BS (1979). Inferences about linkage disequilibrium. *Biometrics* **35**: 235–254.
- Weir BS (1996). *Genetic Data Analysis II: Methods for Discrete Population Genetic Data*. Sinauer Associates: Sunderland, MA, USA.
- Weir BS, Hill WG (1980). Effect of mating structure on variation in linkage disequilibrium. *Genetics* **95**: 477–488.
- Wright S (1931). Evolution in Mendelian populations. *Genetics* **16**: 97.
- Zaykin DV (2004). Bounds and normalization of the composite linkage disequilibrium coefficient. *Genet Epidemiol* **27**: 252–257.

Supplementary Information accompanies this paper on Heredity website (<http://www.nature.com/hdy>)